Acta Geotechnica (2020) 15:1881–1893
https://doi.org/10.1007/s11440-019-00898-4

RESEARCH PAPER

Experimental investigation on physical and mechanical properties of thermal cycling granite by water cooling

Zhennan Zhu[1] · Hong Tian[1] · Gang Mei[2] · Guosheng Jiang[1] · Bin Dou[1]

Received: 3 May 2019 / Accepted: 25 November 2019 / Published online: 6 December 2019

Abstract
Laboratory tests were conducted to study the physical and mechanical properties of granite after heating and water-cooling treatment for 1 and 30 cycles from room temperature to 500 °C. The change mechanisms for the water-cooling treatment were analysed via scanning electron microscope observation. At 500 °C, the volume of granite increases by 1.73% and 2.55%, the mass decreases by 0.16% and 0.31%, and the density decreases by 1.86% and 2.78% after 1 and 30 thermal cycles, respectively. The average values of UCS and E after 1 and 30 cycles both decrease as the temperature rises, while the peak strain exhibits the reverse trend. A yield platform is observed in the yield stage of the stress–strain curve above 300 °C, and the ductility of granite gradually increases with temperature. The normalized P-wave is linear with respect to the normalized UCS and E at 1 thermal cycle, whereas it shows exponential relationships with the normalized UCS and E at 30 thermal cycles. The degradation of the physical and mechanical properties of granite after 1 and 30 cycles is mainly caused by the generation and development of microcracks inside the rock. Compared to 1 thermal cycle, more microcracks are observed at 30 thermal cycles. Therefore, the thermal cyclic treatment can further deteriorate and weaken the physical and mechanical properties of granite.

Keywords Granite · Mechanical properties · Physical properties · SEM · Thermal cycling · Water cooling

1 Introduction

With the continuous increase in population growth and the fast development of the economy, fossil fuels such as coal and oil, with the resulting release of acid rain and greenhouse gases, are becoming increasingly depleted. Clean and efficient energy is the direction of future energy development, for which deep geothermal energy offers substantial advantages in terms of cost, reliability and environmental friendliness [26]. Thus, deep geothermal energy exploitation is now recommended and identified as a renewable and alternative energy source [20]. Aiming to extract deep geothermal energy, the enhanced geothermal system (EGS), which recovers heat from a sufficiently hot thermal reservoir at shallow depth by creating an artificial circulation system, was designed and implemented by Los Alamos National Laboratory in the 1970s [32]. EGS uses hydraulic fracturing and simulation to create highly conductive zones that interconnect an injection well to a production well to form a doublet system [29]. Thermal energy is extracted by circulating water, or another suitable fluid, into the hot fractured rock and pumped to a power plant (binary or flash plant) on the surface to generate electricity [3]. During the exploration of geothermal energy, cold water may be injected and circulated through the fractures in the geothermal reservoirs, which may change the properties of geothermal reservoir rocks (rocks at elevated temperatures) and further influence the stability and safety of the geothermal wellbore wall. Thus, studying the physical and mechanical properties of cyclic heat-treated granite via water cooling is of substantial importance.

Numerous laboratory studies on various types of rocks, such as granite [6, 7, 36, 46, 54], marble [27, 28, 33], sandstone [24, 25, 38, 47, 48], limestone [14, 27, 49, 51]

✉ Hong Tian
htian@cug.edu.cn

[1] Faculty of Engineering, China University of Geosciences, Lumo Road 388, Wuhan 430074, China

[2] School of Engineering and Technology, China University of Geosciences, Xueyuan Road 29, Beijing 100083, China

and claystone [39], that have been exposed to high temperatures have been conducted to investigate the effects of high temperature on the physical and mechanical properties of rocks and their the microstructures. In the terms of rock physical properties, the volume, porosity, permeability and electrical conductivity of rocks increase with the thermal temperature, while the density, wave velocity and thermal conductivity typically decrease. The mechanical properties mainly focus on strength and deformation characteristics, such as compressive stress, tensile stress, elastic modulus and post-peak characteristics. The tensile strength, compressive strength and elastic modulus gradually decrease with the temperature and exhibit various levels of deterioration. The rocks after high-temperature treatments are less brittle and exhibit much stronger ductile characteristics compared to those without treatment. Scanning electron microscopy (SEM) [4, 7, 47], optical microscopy [28, 34] and X-ray microcomputed tomography (CT) [11, 22, 53] analyses were conducted to identify the change mechanisms of rock physical and mechanical properties after exposure to high temperature.

Deep granite reservoirs have adequate temperatures for serving as geothermal reservoirs, according to exploratory geothermal well tests [12]. Although the influences of high temperature on granite physical and mechanical properties have been investigated systematically as discussed above, the granites in most of the previous studies were cooled naturally to room temperature inside or outside of the furnace; hence, those studies are not applicable to geothermal energy extraction/EGS. Meanwhile, only a few experiments have captured the effect of the cyclic natural cooling treatment on granite physical and mechanical properties [22, 34] and limited research has been conducted on heat-treated granite via water cooling [18, 21, 36]. Recently, Xu and Sun [43] have investigated effects of quenching cycle on tensile strength of granite with water cooling and found that the static tensile strength decreases with increasing temperature and increasing number of quenching cycles. Ge and Sun [13] and Zhu et al. [56] studied the damage of granite after cyclic heating and cooling with circulating water by acoustic emission (AE) and found that the AE curve agrees well with the stress–time curve at each test temperature point and can reflect the mechanical damage increasing with the increase in water cooling at high-temperature cycles. However, to the authors' knowledge, the microscopic change mechanisms of granite mechanical properties under cyclic heating and water cooling have not been published. In the presented study, granite material is used to study the physical (weight, volume, density and P-wave velocity) and mechanical properties (strength, deformation and failure behaviours) of rock after heating and water-cooling treatment for 1 and 30 cycles. According to a comprehensive review of international literature, the effects of cyclic water cooling on mechanical properties of granite are analysed, and the relations between the physical and mechanical properties of water-cooled granite are also discussed. Then, the microscopic mechanism of heating and water cooling on the physical and mechanical behaviours of the tested granite was revealed based on SEM analysis. Therefore, the objectives of this paper are to investigate the effects of the cyclic heating and water-cooling processes on both the physical and mechanical properties of granite and to identify the microscopic change mechanisms based on SEM observations. This study is expected to support analytical calculations and numerical simulations in geothermal energy extraction.

2 Experimental design

2.1 Description of rock specimens

Gray and fine-grained granite blocks were collected from a mine in Suizhou city, Hubei province, China. According to the method that is suggested by the International Society for Rock Mechanics (ISRM) [10], cylindrical specimens with a diameter of 50 mm and a height of 100 mm were machined from the same block (Fig. 1). The natural density of the specimens is 2.603 g/cm^3, and the average longitudinal wave velocity is 3770 m/s. Petrophysical analysis with X-ray diffraction demonstrates that the main mineral components of the granite are 77.68% feldspar, 10.58% quartz, 6.28% biotite, 3.24% chlorite and 2.22% amphibole.

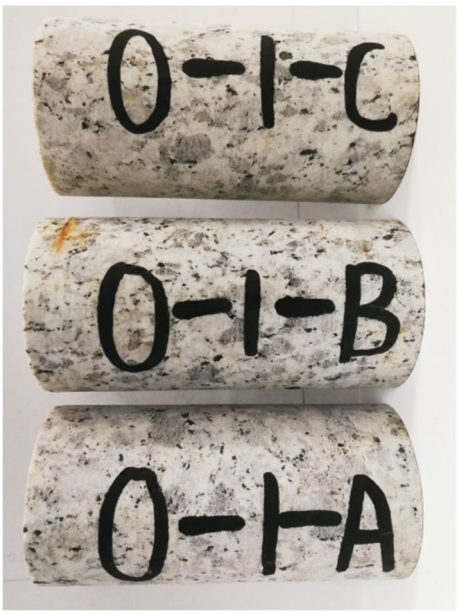

Fig. 1 Untreated granite specimens

2.2 Experimental procedure

The procedures of the present experiment are illustrated in Fig. 2. All the specimens were initially subjected to dry processing, which is performed by placing the specimens in a drying oven that is maintained at 105 °C for 24 h to remove all moisture content to eliminate the effect of the natural water content on the experimental results. The quality, size and longitudinal wave velocity of each specimen were measured with a Vernier calliper, an electronic balance and an RSM-SY5 (T) ultrasonic concrete tester, respectively. Any specimen with an abnormal density or a wave velocity was abandoned to ensure the reliability of the test results. The remaining specimens were divided into nine groups, with 4 specimens in each group (three for mechanical testing and one for making thin slices for SEM observation), including a control group, which was not subjected to thermal treatment. The specimens were heated in the SG-XL1200 high-temperature box furnace to the predetermined testing temperatures (150, 300, 400 and 500 °C) using a modest heating rate of 5 °C/min, as in the previous experiments on rocks [4, 27, 38, 46, 49]. Then, specimens were maintained at the predetermined temperatures for 2 h to ensure that all the specimens had been adequately heated. Once the constant temperature stage was over, the tested specimens were cooled via water immersion in a water bath with a sufficient volume of distilled water. After the specimens had cooled to room temperature, they were subjected to dry processing again, which is regarded as one thermal cycle. Then, the diameter, height, mass and wave velocity of each specimen after the thermal cycle were measured once again. To investigate the effects of thermal cycles on granite physical and mechanical properties, half of the specimens were subjected to 30 thermal cycles and the quality, size and longitudinal wave velocity of each specimen were measured after each thermal cycle.

The microstructural characteristics of the specimens after heating and water-cooling treatment were observed using a Quanta250 SEM, and uniaxial compression tests were conducted using a TAW-2000 electro-hydraulic servo-controlled rock mechanics testing system in displacement-controlled conditions at a rate of 0.3 mm/min. A separate group of natural granite specimens without heat treatment were also tested for reference. The test results of the granite physical and mechanical properties before and after high-temperature treatment are listed in Table 1.

3 Experimental results

3.1 Volume, mass and bulk density

To more accurately characterize the change laws of the mass, volume and bulk density with the temperature of the granite after heating and water-cooling treatment, the volume increase rate (η_v), mass decrease rate (η_m) and density

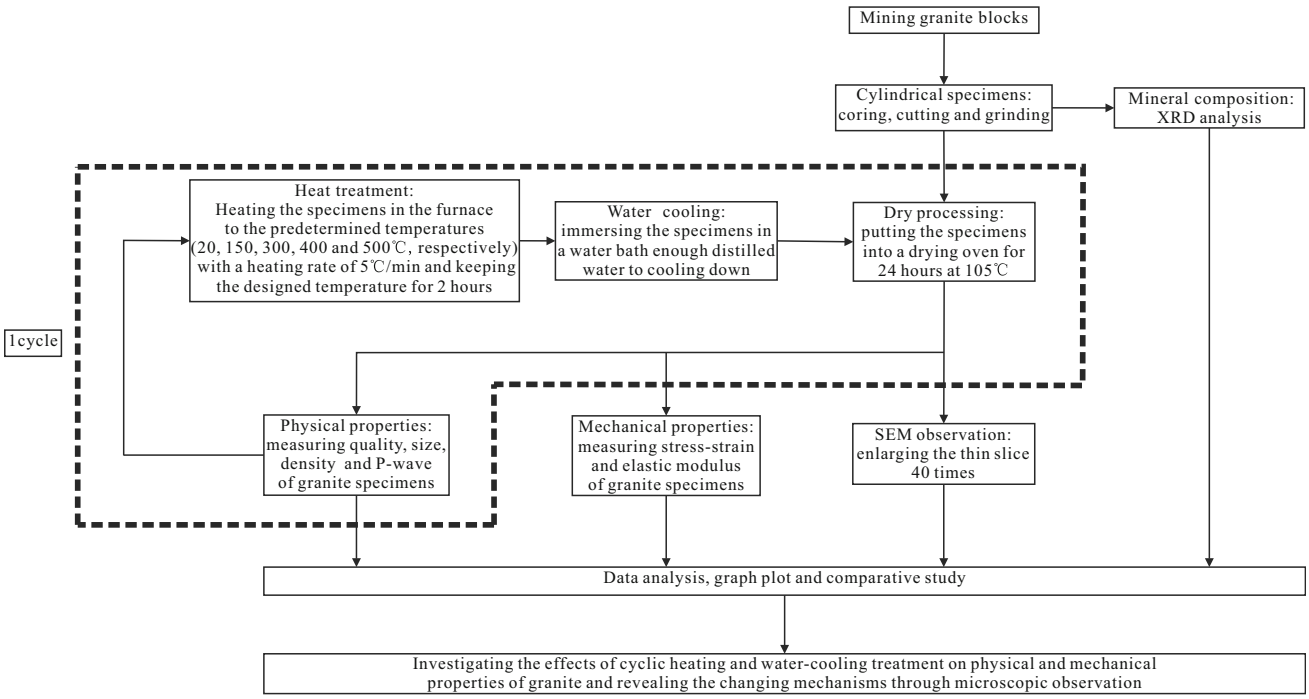

Fig. 2 Test flow chart

Table 1 Physical and mechanical parameters of water-cooling-treated granite after exposure to various temperatures

Number	T (°C)	V_1 (cm^3)	V_2 (cm^3)	m_1 (g)	m_2 (g)	ρ_1 (g/cm^3)	ρ_2 (g/cm^3)	V_{p1} (m/s)	V_{p2} (m/s)	UCS (MPa)	E (GPa)	ε_s (%)
0-1-A	20*	188.11	188.11	502.28	502.28	2.670	2.670	3812	3812	110.09	17.87	0.86
0-1-B	20*	190.05	190.05	507.24	507.24	2.669	2.669	3873	3873	120.16	17.77	0.86
0-1-C	20*	189.27	189.27	504.86	504.86	2.667	2.667	3737	3737	125.40	19.53	0.82
1-1-A	150	188.05	188.40	488.07	487.67	2.595	2.588	3759	3127	104.99	16.54	0.88
1-1-B	150	188.32	188.46	489.46	489.07	2.599	2.595	3846	3336	102.98	16.76	0.91
1-1-C	150	189.88	190.50	491.88	491.45	2.590	2.580	3831	3365	107.35	17.27	0.92
1-5-A	150	184.63	185.74	479.96	479.38	2.599	2.581	3615	2885	61.37	5.52	1.45
1-5-B	150	184.89	186.06	480.69	480.10	2.600	2.580	3823	2943	66.43	5.38	1.48
1-5-C	150	185.72	186.77	484.74	484.14	2.610	2.592	3887	2580	63.52	5.76	1.47
2-1-A	300	194.43	195.87	505.58	505.01	2.600	2.578	3774	2525	99.77	13.71	0.96
2-1-B	300	194.27	195.24	503.29	502.81	2.591	2.575	3774	2489	95.08	15.15	0.94
2-1-C	300	194.82	196.33	506.56	506.02	2.600	2.577	3745	2516	97.08	14.05	0.94
2-5-A	300	194.09	196.25	506.34	505.49	2.609	2.576	3823	1974	49.04	4.77	1.51
2-5-B	300	193.15	195.62	501.63	500.79	2.597	2.560	3799	2098	48.89	4.73	1.50
2-5-C	300	194.30	196.41	507.24	506.54	2.611	2.579	3831	2114	44.46	4.27	1.53
3-1-A	400	188.11	190.38	489.37	488.80	2.601	2.568	3623	1961	91.48	13.97	0.99
3-1-B	400	188.86	191.03	482.76	482.21	2.556	2.524	3937	2069	89.55	13.13	0.96
3-1-C	400	196.13	198.57	505.96	505.32	2.580	2.545	3650	2143	87.85	13.45	1.03
3-5-A	400	193.15	196.92	506.47	505.29	2.622	2.566	3615	1310	43.82	4.12	1.65
3-5-B	400	191.56	195.32	494.91	493.93	2.584	2.529	3704	1376	42.60	4.18	1.54
3-5-C	400	194.55	198.23	508.25	507.11	2.612	2.558	3615	1422	40.66	4.13	1.66
4-1-A	500	194.29	197.66	507.18	506.43	2.610	2.562	3788	1613	82.00	12.02	1.07
4-1-B	500	189.50	192.95	492.82	492.02	2.601	2.550	3984	1530	74.57	10.49	1.12
4-1-C	500	195.71	198.90	506.02	505.13	2.585	2.540	3846	1658	80.41	11.70	1.06
4-5-A	500	185.75	190.39	486.51	484.74	2.619	2.546	3707	648	25.13	2.07	2.13
4-5-B	500	194.14	199.19	505.88	504.36	2.606	2.532	3701	826	25.55	2.25	2.22
4-5-C	500	195.22	200.20	506.54	505.26	2.595	2.524	3704	1091	24.33	2.07	2.19

*Expressed as room temperature

decrease rate (η_ρ) are introduced, which are, respectively, defined as follows:

$$\eta_v = \frac{V_a - V_0}{V_0} \times 100\% \quad (1)$$

$$\eta_m = \frac{m_0 - m_a}{m_0} \times 100\% \quad (2)$$

$$\eta_\rho = \frac{\rho_0 - \rho_a}{\rho_0} \times 100\% \quad (3)$$

where V_0, m_0 and ρ_0 denote the volume, mass and density, respectively, of the specimen prior to thermal treatment and V_a, m_a and ρ_a denote the volume, mass and density of the specimen after heating and water-cooling treatment.

As shown in Fig. 3, the average η_v of 1 cycle increases linearly with the temperature and it increases to 1.73% at 500 °C. The average value of η_v over 30 cycles increases exponentially with the temperature and accelerates substantially above 300 °C. The average value of η_v over 30

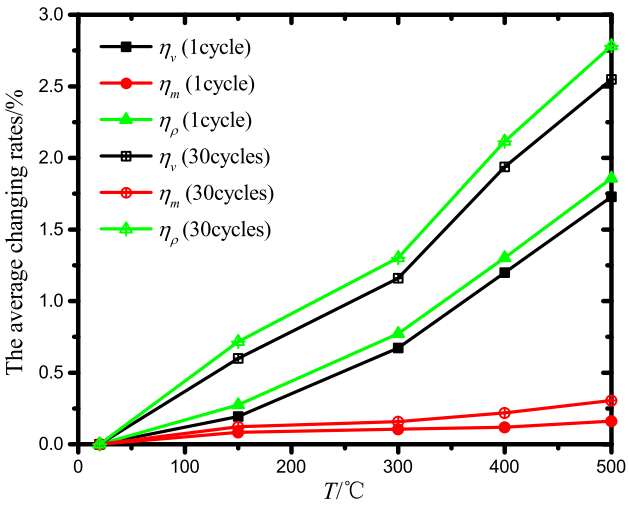

Fig. 3 Relationships between temperature and the average change rates of volume, mass and bulk density

cycles is 1.16% at 300 °C, and it increases to 1.94% and 2.55% at 400 °C and 500 °C, respectively. The average value of η_m also increases with the thermal temperature; however, the average values of η_m over 1 and 30 cycles only increase to 0.16% and 0.31% at 500 °C. Compared to the volume increase rates, the mass decrease rates are smaller; thus, the trends of the density decrease rate and the volume increase rate with temperature are highly similar below 500 °C. The average value of η_ρ over 30 cycles increases with temperature; at 150 °C, η_ρ is only 0.72%, while it reaches 1.30%, 2.12% and 2.78% at 300 °C, 400 °C and 500 °C, respectively.

3.2 P-wave velocity

The P-wave velocity of each specimen for each desired thermal cycle was measured to investigate the effect of thermal cycling on granite specimens after water-cooling treatment. The variations of the P-wave velocity with the number of thermal cycles are presented in Fig. 4. The P-wave velocities of granite after treatment at high temperatures exhibit a similar trend. Most of the decrease in the P-wave velocity occurred within 5 thermal cycles, especially after the first cycle. Afterwards, the P-wave velocities changed little with the number of thermal cycles. In addition, the P-wave velocity decreases with the thermal temperature. The values of the P-wave velocity of 30 cycles decrease by 74.4%, 54.0%, 37.6% and 23.4% at 150 °C, 300 °C, 400 °C and 500 °C, respectively.

3.3 Stress–strain curves

As shown in Fig. 5, the stress–strain curves for the specimens after heating and water-cooling treatment for 1 and 30 cycles exhibit four stages: compaction, elastic deformation, yield and failure. According to Fig. 5, the strength and deformation behaviour of granite depend strongly not only on the heating and water-cooling treatment but also on the number of cycles. In the compaction stage, all the curves display a concave-up shape from the start of the test and the nonlinearity in this stage increases with the thermal temperature for both 1 and 30 cycles, which is likely the result of more thermal cracks being induced by higher-temperature treatments. The slope of the curve in the elastic deformation stage decreases with the increase in the temperature of the heating treatment, especially for 30 cycles. Meanwhile, a yield platform can be observed in the yield stage above 300 °C for both 1 and 30 cycles; hence, the brittleness of the granite gradually decreases and the ductility gradually increases as the temperature rises. When exposed to a higher thermal temperature after water-cooling treatment, the granite specimens fail more slowly after the peak strength with increasing axial deformation.

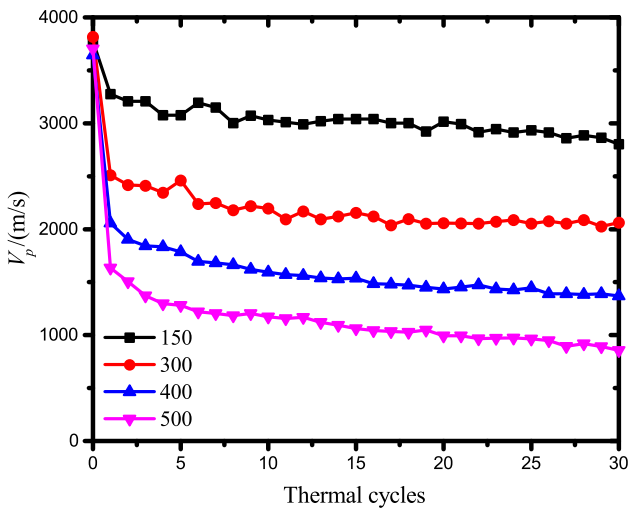

Fig. 4 Relationship between the number of thermal cycles and the P-wave velocity of granite after heating and water-cooling treatment

3.4 Rock strength and deformation behaviour

The relationships between the temperature and the mechanical parameters of granite after heating and water-cooling treatment for 1 and 30 cycles are plotted in Fig. 6. Both the uniaxial compressive strength (UCS) and the elastic modulus (E) decrease with the heating temperature. Prior to the thermal treatments, the average values of UCS and E were 118.55 MPa and 18.39 GPa, respectively, which decreased to 105.11 MPa and 16.86 GPa at 150 °C after the first thermal cycle. However, the average UCS and E values decreased to 63.78 MPa and 5.55 GPa even at 150 °C when the number of thermal cycles increased to 30. The thermal cycling after water-cooling treatment had a substantial effect on the granite mechanical properties. The values of UCS decreased by 33.37% and 78.91% at 500 °C after 1 and 30 thermal cycles, respectively, and the values of E decreased by 38.82% and 88.42% at 500 °C after 1 and 30 thermal cycles, respectively. According to Fig. 6, the average peak strain (ε) increases with the thermal temperature and changes dramatically after 30 thermal cycles, which accords with the trends of UCS and E versus the heating temperature.

3.5 Microscopic observation

Thin sections of the water-cooling-treated granite specimens before and after thermal treatments of 1 and 30 cycles were enlarged by a factor of 40 and observed via SEM. As shown in Fig. 7a, mineral grains are arrayed closely and few initial pores and fissures can be observed in the specimen without heating. After the first thermal cycle, when the temperature is increased to 150 °C, we observe a

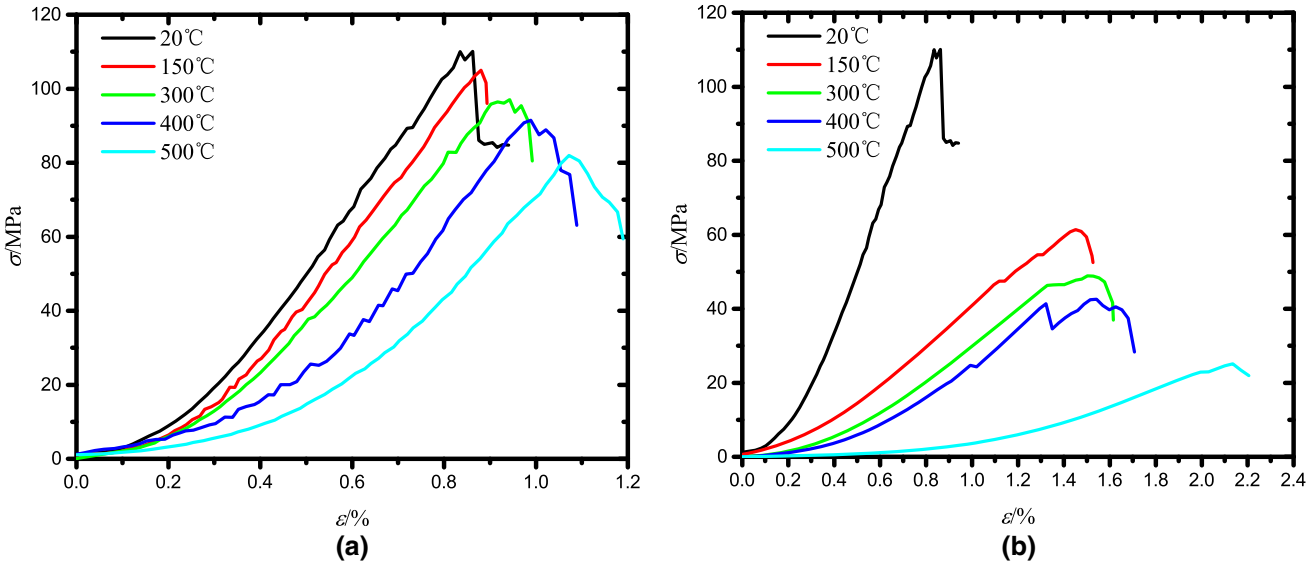

Fig. 5 Stress–strain curves for high-temperature granite with the water-cooling treatment: **a** one thermal cycle and **b** 30 thermal cycles

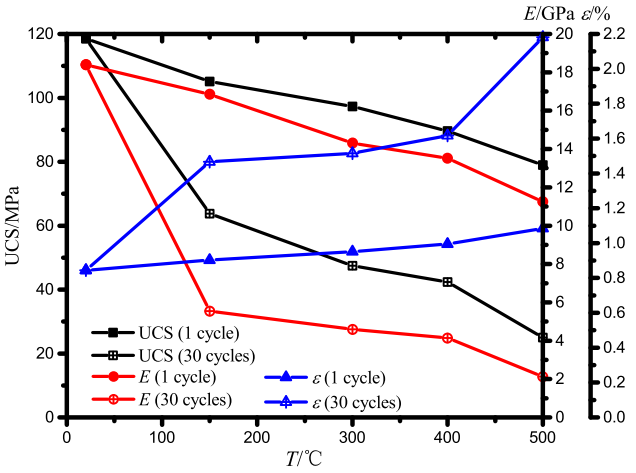

Fig. 6 Relationships between temperature and granite mechanical parameters

few microstructural alterations compared with the result at normal temperature in Fig. 7b. Increasingly many thermal microcracks are induced with the gradual increase in the temperature to 500 °C (Fig. 7c–e). After 30 thermal cycles, many microcracks are observed, even at 150 °C (Fig. 7f), and the crack density of granite at 30 thermal cycles is substantially higher than that at 1 thermal cycle. Many microcracks in the 300 °C and 400 °C specimens have begun to interact and coalesce with each other (Fig. 7g–h), which leads to the further increase in the crack density compared to the specimens at 1 thermal cycle. Finally, a microcrack network is formed in the thin section of the specimen at 500 °C (Fig. 7i).

Chen et al. [4] and Yang et al. [46] observed that no microcracks can be found inside the granite specimen after thermal heating to 200 °C with natural cooling. However, in the current study, a few microcracks are observed after heating to 150 °C with water-cooling treatment. In addition, according to Chen et al. [4], a microcrack network is formed in thin sections of the specimen above 573 °C and for the heat-treated granite specimens that are subjected to water cooling, a microcrack network is formed in the thin section of each specimen at 500 °C after 30 thermal cycles. Thus, it is concluded that cyclical water-cooling treatment can induce microcracks more easily and induces more severe thermal damages to granite compared with natural cooling treatment.

To quantify the microcracks inside the granite specimens after heating and water-cooling treatment for 1 and 30 cycles, the microcrack density (ρ_f) is defined as follows:

$$\rho_f = \frac{L}{S} \tag{4}$$

where ρ_f is the microcrack density that is measured in the thin section of the specimen after thermal treatment; L represents the total length of the microcrack that is observed in the thin section of the specimen after thermal treatment; and S represents the area of the thin section of the specimen.

The use of methods of damage mechanics to study rock thermodynamics is a new strategy in rock mechanics [24]. Thermal damage variables D_{VT} and D_{ET} are introduced for quantifying the damage degree of granite specimens after heating and water-cooling treatment for 1 and 30 cycles, which are defined as follows:

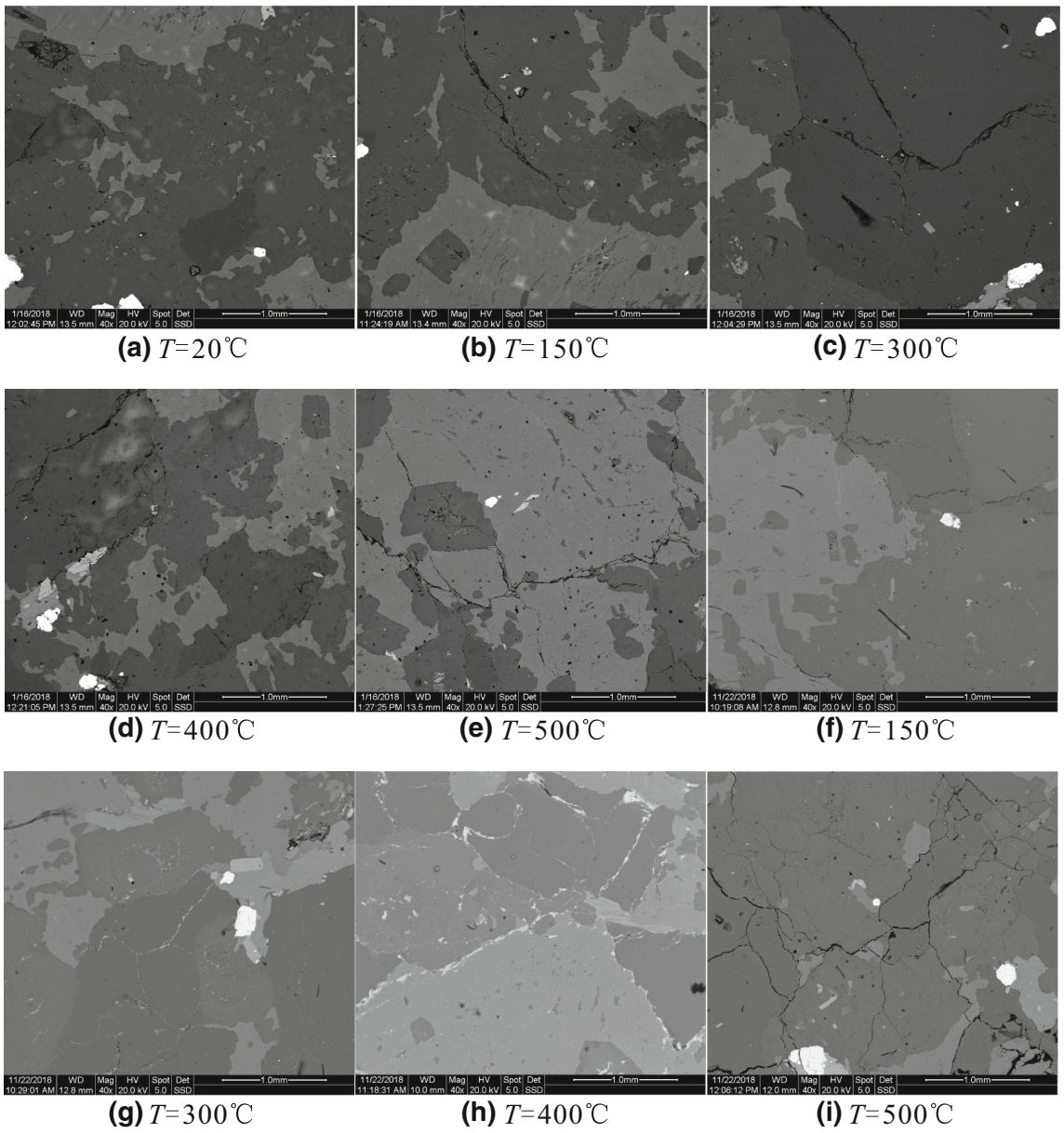

Fig. 7 SEM images of water-cooling-treated granite after heating to various temperatures: 1 cycle: **b–e**; 30 cycles: **f–i**

$$D_{VT} = 1 - \left(\frac{V_T}{V_0}\right)^2 \tag{5}$$

$$D_{ET} = 1 - \frac{E_T}{E_0} \tag{6}$$

where D_{VT} and D_{ET} are the thermal damage variables; V_T and E_T represent the longitudinal wave velocity and the elastic modulus, respectively, of granite after heating and water-cooling treatment; and V_0 and E_0 represent the longitudinal wave velocity and the elastic modulus, respectively, of granite without thermal treatment.

The values of the microcrack density and the thermal damage variable are listed in Table 2. Figure 8 displays the relationships between the temperature and the microcrack density and thermal damage variable. Thermal damage accords with the microcrack density after 1 and 30 cycles. The values of microcrack density after 30 cycles (15.253, 18.491, 22.260 and 30.204 mm/mm^2) are higher than those after 1 cycle (6.799, 10.310, 13.637 and 18.021 mm/mm^2). The values of D_{VT} and D_{ET} exhibit a similar trend to the thermal temperature after 1 and 30 cycles. The values of D_{ET} after 30 cycles are larger than the values of D_{VT} after 30 cycles, while the values of D_{ET} after 1 cycle are smaller than the values of D_{VT} after 1 cycle; hence, the heating and water-cooling treatment may have little effect on the physical and mechanical properties.

Table 2 Microcrack density and the thermal damage variable of granite after heating and water-cooling treatment

T (°C)	ρ_f (mm/mm^{-2})		V_T (m/s)		D_{VT}		E_T (GPa)		D_{ET}	
	1 cycle	30 cycles	1 cycle	30 cycles	1 cycle	30 cycles	1 cycle	30 cycles	1 cycle	30 cycles
20	1.287	1.287	3807	3807	0.000	0.000	18.39	18.39	0.000	0.000
150	6.799	15.253	3276	2802	0.260	0.458	16.86	5.55	0.160	0.909
300	10.310	18.491	2510	2062	0.565	0.707	14.30	4.59	0.395	0.938
400	13.637	22.260	2058	1370	0.708	0.871	13.52	4.15	0.460	0.949
500	18.021	30.204	1600	855	0.823	0.950	11.25	2.13	0.626	0.987

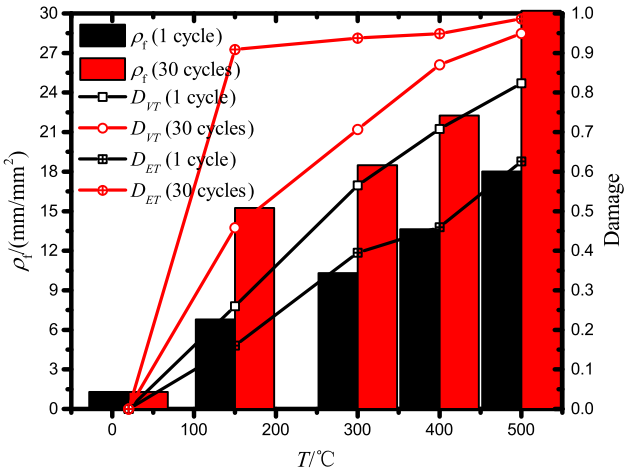

Fig. 8 Relationships between the temperature and the microcrack density and thermal damage variable of granite after heating and water-cooling treatment for 1 and 30 cycles

3.6 Macroscopic failure modes

The macroscopic failure modes of granite after heating and water-cooling treatment for 1 and 30 cycles are presented in Fig. 9. When there is no thermal damage, the granite is a typically brittle rock material and shows a multiple axial splitting tensile failure mode. As the applied temperatures increase to 150 and 300 °C for 1 cycle, there is a tendency to transition from axial splitting to shear failure. From 400 °C onward, a through-going shearing plane emerges in the granite specimens and the granite exhibits a macroscopic shear failure mode, which is consistent with the previous observations [40]. After 30 thermal cycles, the integrity of specimen is lower than after treatment for 1 thermal cycle. According to Rong et al. [34], this is because more thermally induced microcracks developed in specimens that were subjected to more thermal cycles. After heating at 150 and 300 °C, the specimens show two parallel shear planes, which represent double parallel shear plane failure. Above 400 °C, a single shear failure plane occurs in the specimens and the angle of the failure plane is higher than that after 1 thermal cycle. In summary, the heating and water-cooling treatment and the number of thermal cycles both substantially influence the failure mode of granite.

4 Discussion

4.1 Influence mechanism of high temperature

The increase in the volume, the decrease in the wave velocity and the deterioration of mechanical properties are closely related to the generation and development of microcracks. Granite mineral grains will expand after heating treatment, and the heating temperature may have a substantial effect on the structure of the granite specimens. Differences in the thermal-expansion characteristics of among the minerals in the assemblage of mineral grains can cause structural damage upon heating the granite. In addition, differences in thermal expansion along the crystallographic axes of the same mineral can also cause structural damage upon heating [8]. Thus, microdefects will be produced between mineral grain boundaries or inside mineral grain bodies, and the higher the thermal temperature is, the more microdefects are produced (Fig. 7). Meanwhile, the states of water form water vapour and escape from the microcracks, thereby causing high air pressure which intensifies the formation and expansion of microcracks and micropores [50]. Due to severe deformation and microcracks, the original mineral structures will be destroyed and irrecoverable deformation will be produced, even after cooling to room temperature [39]. In addition, the open microcracks in granites that are caused by thermal treatment will rapidly close under a minor load; as a result, the brittleness of granite gradually decreases and the ductility gradually increases as the temperature rises [46].

The mass decrease of granite after temperature change is mainly caused by the loss of various types of water in the temperature range that is studied in this research (20–500 °C). The temperature ranges of vaporization of attached water, bound water and constitution water are

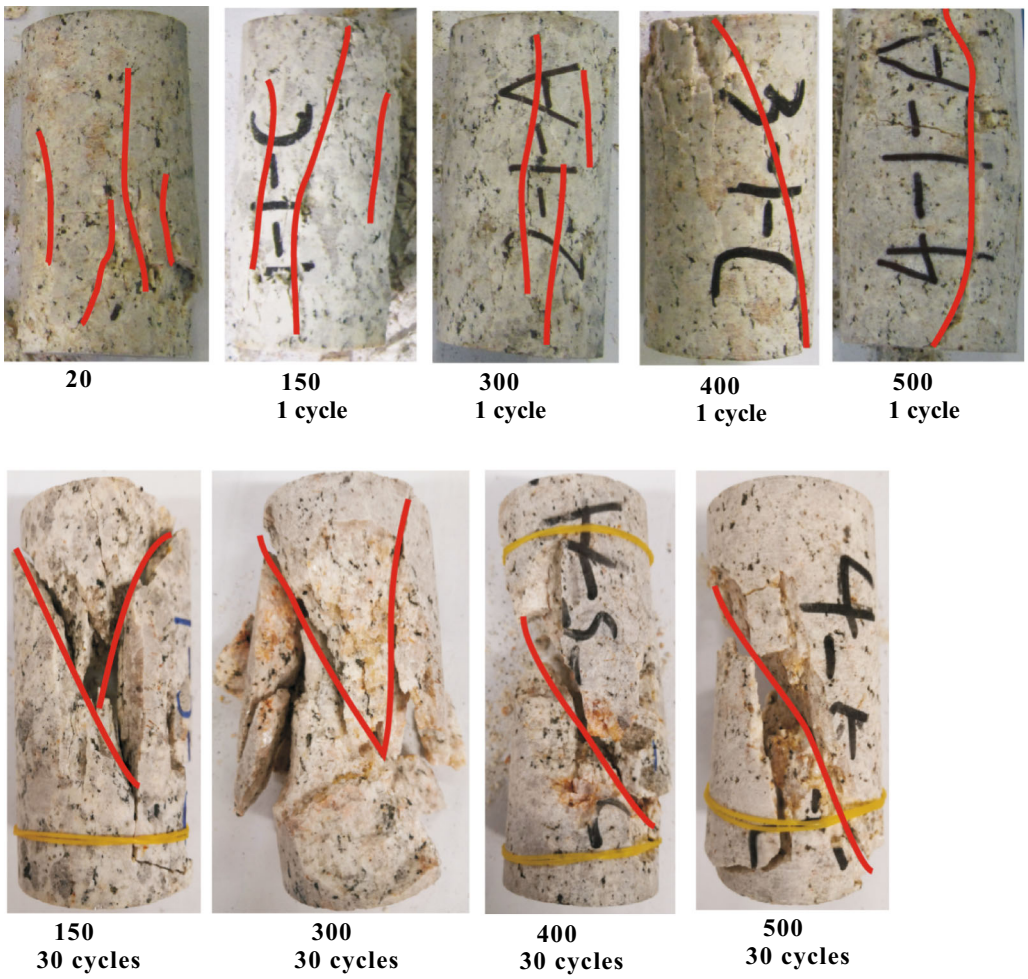

Fig. 9 Macrofractures of granite after heating and water-cooling treatment for 1 and 30 cycles

room temperature to 100 °C, 100–300 °C and 300–500 °C, respectively [25]. The average mass decrease rate increases gradually with the thermal temperature (Fig. 3); hence, the higher the temperature the granite experiences, the greater the loss of granite. According to the above analysis, the granite mass decreases with temperature, while the granite volume increases with temperature. Consequently, the granite density decreases with temperature and the change amplitude increases with temperature.

It is concluded that the values of P-wave, UCS and E of the granite specimens after heating and water-cooling treatment all decrease with the temperature, which is attributed to the production and development of microcracks. Therefore, the changes of the physical and mechanical properties after high-temperature treatments must be related. The relationships between the normalized V_{pT}/V_{p0} values and the normalized UCS_T/UCS_0 and E_T/E_0 values of the heat-treated granite by water cooling for 1 and 30 cycles are plotted in Figs. 10 and 11, respectively. Via fitting analysis of the above experimental data, normalized V_{pT}/V_{p0} is linear with respect to normalized UCS_T/UCS_0

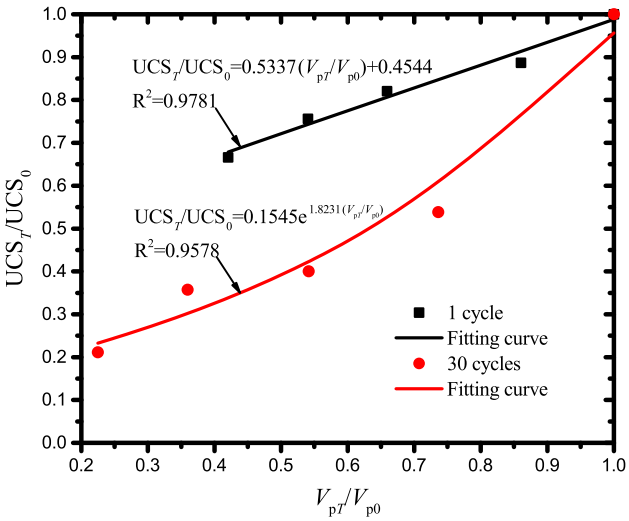

Fig. 10 Relationships between the normalized P-wave velocity and the normalized uniaxial compressive stress of water-cooled granite

and E_T/E_0 after the first thermal cycle and exhibits exponential relationships with normalized UCS_T/UCS_0 and $E_T/$

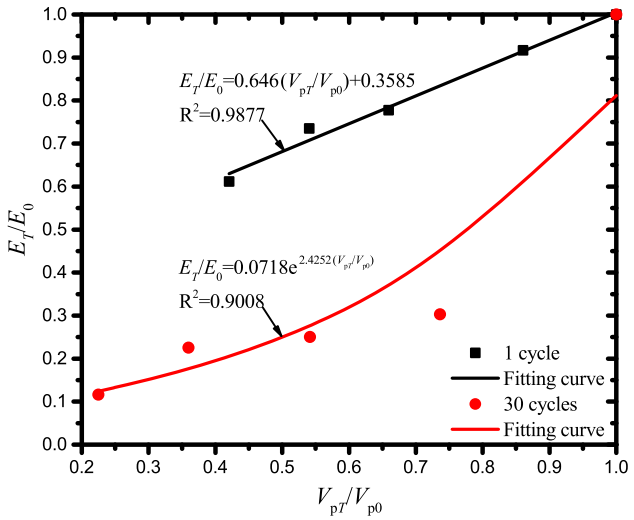

Fig. 11 Relationships between the normalized P-wave velocity and the normalized elastic modulus of water-cooled granite

E_0 after 30 thermal cycles. Moreover, the experimental properties of granite at 30 thermal cycles change more intensely than those at 1 thermal cycle. The fitting results are presented in Table 3, and the correlation coefficients of the fitting curves all exceed 0.9008; hence, there are strong links between the changes of the wave velocity and UCS and E of the granite after heating and water-cooling treatment for 1 and 30 thermal cycles.

4.2 Influence mechanism of cyclic water cooling

Normalized values of the uniaxial compressive stress (UCS_T/UCS_0) and the elastic modulus (E_T/E_0) of granites at various temperatures are collected from a comprehensive review of the international literature, which includes Chinese publications that are not yet available for the English-speaking scientific community. The values of UCS_T/UCS_0

Table 3 Relationships between the normalized wave velocity and the normalized uniaxial compressive stress and the elastic modulus of water-cooled granite

Thermal cycle	Fitting curves	R^2
1	$UCS_T/UCS_0 = 0.5337(V_{pT}/V_{p0}) + 0.4544$	0.9781
30	$UCS_T/UCS_0 = 0.1545\exp[1.8231(V_{pT}/V_{p0})]$	0.9578
1	$E_T/E_0 = 0.646(V_{pT}/V_{p0}) + 0.3585$	0.9877
30	$E_T/E_0 = 0.0718\exp[2.4252(V_{pT}/V_{p0})]$	0.9008

V_{pT}, UCS_T and E_T represent the values of the P-wave, uniaxial compressive stress and elastic modulus of granite that are measured and calculated after treatment at various temperatures; V_{p0}, UCS_0 and E_0 represent the values of the P-wave, uniaxial compressive stress and elastic modulus of granite that are measured and calculated at normal temperature

and E_T/E_0 that were obtained for granites after heating and water-cooling or air-cooling treatment are presented in Figs. 12 and 13, respectively. The experimental data of Kumari et al. [21] and Xi et al. [42] were collected from heat-treated granite by water cooling, and "Average" represents the average values of UCS_T/UCS_0 and E_T/E_0 at each temperature for all heat-treated granites via natural cooling. Below 500 °C, the changes in UCS_T/UCS_0 and E_T/E_0 of the heat-treated granites by water cooling are larger than those of the heat-treated granites by natural cooling. At 400 °C, the average UCS_T/UCS_0 and E_T/E_0 values of the heat-treated granites by natural cooling are 0.94 and 0.91, while the UCS_T/UCS_0 and E_T/E_0 values by water cooling after the first thermal cycle in this paper decrease to 0.76 and 0.74, respectively, and the UCS_T/UCS_0 and E_T/E_0 values at 30 thermal cycles are only 0.36 and 0.23. When the temperature is increased to 500 °C, the UCS_T/UCS_0 and E_T/E_0 values at 1 thermal cycle that are obtained in this paper decrease by 33% and 0.61, respectively, and the UCS_T/UCS_0 and E_T/E_0 values at 30 thermal cycles decrease by 79% and 88%.

Therefore, both the water-cooling and thermal cycling treatments substantially influence the granite physical and mechanical properties. The temperature decrease rate of heat-treated granites by water cooling is much more rapid than that by air cooling and causes more intense and sudden thermal shock [35]. This thermal shock further widens the cracks that have developed in the sample; thus, high

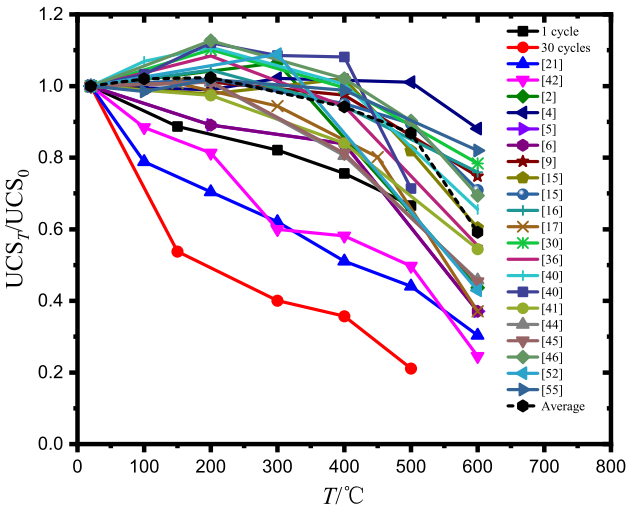

Fig. 12 Relationships between the temperature and the normalized uniaxial compressive stress of water-cooling- and natural-cooling-treated granites after being heated to various temperatures ("1 cycle" and "30 cycles" represent the values of UCS_T/UCS_0 that were obtained in this study; "[21, 42]" represent the values of UCS_T/UCS_0 of granite specimens after heating and water-cooling that were obtained from references; "[2–55]" represent the values of UCS_T/UCS_0 of granite specimens after heating and air-cooling treatment that were obtained from references; and "Average" represents the average value of UCS_T/UCS_0)

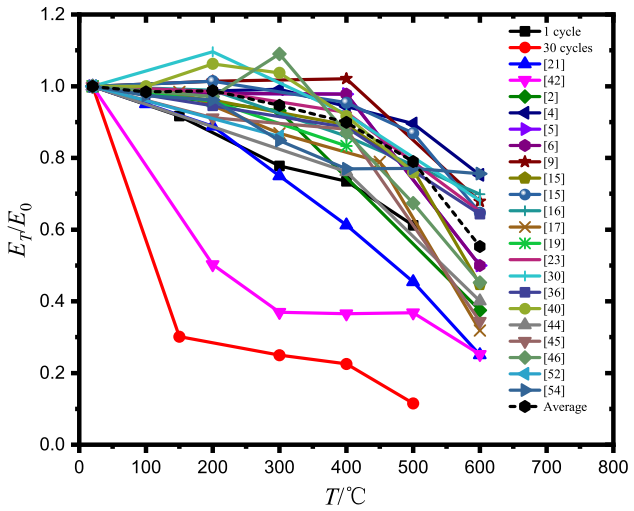

Fig. 13 Relationships between the temperature and the normalized elastic modulus of water-cooling- and natural-cooling-treated granites after being heated to various temperatures ("1 cycle" and "30 cycles" represent the values of E_T/E_0 obtained in this study; "[21, 42]" represent the values of E_T/E_0 of granite specimens after heating and water-cooling that were obtained from references; "[2–54]" represent the values of E_T/E_0 of granite specimens after heating and air-cooling treatment that were obtained from references; and "Average" represents the average value of E_T/E_0)

cooling rates or more rapid and larger temperature reductions enhance thermally induced pre-fractures, thereby resulting in visible macroscale cracks in the rock mass [31]. In addition, for heat-treated granite specimens by water cooling, water will intrude into the granite bodies through the microcracks and micropores that are produced by heating and the strong contract among mineral grains will be further jeopardized, which will intensify the propagation and development of microdefects [21]. As a result, the mechanical properties of granites after heating and water-cooling treatment will be further deteriorated and weakened. Moreover, as shown in Fig. 7, thermal cycling treatment will cause a further change in the microstructure of the granite specimens [22, 34] and will lead to huge degradations in the physical and mechanical properties of granites after 30 thermal cycles.

4.3 Implications for geothermal energy exploitation

During long-term water circulation for exploiting deep geothermal energy, the hot geothermal reservoir rocks will be inevitably subjected to cyclic rapid temperature changes [3]. The above analysis suggests that further deteriorations of the mechanical properties were induced by rapid temperature reductions during cyclic water cooling. As a result, the deterioration of the mechanical properties tends to cause instability of the wall rock. Cooling may induce a pervasive tensile microcracking process prior to macroscopic failure location [1], which ultimately results in wall rock breakouts [37]. The experimental results demonstrated the substantial effect of the cyclic rapid cooling treatment and provided reliable parameter values for the accurate simulation of wellbore stability. In addition, the exploitation of geothermal energy entails the use of hydraulic fracturing and simulation to create highly conductive zones that interconnect an injection well to a production well [29] and hydraulic stimulation of a geothermal reservoir is a coupled process of thermal microcracking and hydraulic fracturing [18]. Considering the deterioration of the mechanical properties of geothermal reservoir rocks that is caused by cyclic rapid water cooling, it is beneficial for well drilling and producing fracture systems in geothermal reservoirs.

5 Conclusions

The physical and mechanical properties of granite after heating and water-cooling treatment for 1 and 30 cycles were studied experimentally, and the change mechanisms were identify via the SEM image analyses. Based on an extensive review of the mechanical properties of granites after high-temperature treatment, the following conclusions are drawn:

After heating and water-cooling treatment, the volume of granite increases with the temperature, the mass and the density of granite decrease with the temperature, and the changes in these quantities increase with the temperature. At 500 °C, the volume of granite increases by 1.73% and 2.55%, the mass of granite decreases by 0.16% and 0.31%, and the density of granite decreases by 1.86% and 2.78% over 1 and 30 thermal cycles, respectively.

The average values of UCS and E of granite after heating and water-cooling treatment for 1 and 30 cycles decrease as the temperature increases, while the peak strains exhibit the reverse trend. The decrease extents of UCS and E of the heat-treated granites by water cooling are larger than those of the heat-treated granites by natural cooling due to considerable thermal damage that is caused by intense thermal shock and water intrusion. A yield platform appears in the yield stage of the stress–strain curve above 300 °C, and the ductility of granite gradually increases as the temperature rises.

The average P-wave velocities of the heat-treated granite by water cooling for 1 and 30 cycles decrease with temperature and they decrease by 58.6% and 76.6%, respectively, at 500 °C. The normalized P-wave is linear with respect to the normalized UCS and E after first thermal cycle and shows exponential relationships with the normalized UCS, E after 30 thermal cycles.

According to microscopic observation of the thin sections of the water-cooling-treated granite specimens after thermal treatments of 1 and 30 cycles, the deterioration of the physical and mechanical properties of granite is mainly due to the generation and development of microcracks inside the specimen. Based on the observation of more microcracks at 30 thermal cycles than at 1 cycle, the thermal cycling treatment can further deteriorate and weaken the granite physical and mechanical properties.

Acknowledgements This work is jointly supported by National Natural Science Foundation of China (Nos. 41602374 and 41674180) and the Fundamental Research Funds for the Central Universities-Cradle Plan for 2017 (Grant No. CUGL170207).

Compliance with ethical standards

Conflict of interest The authors declared that they have no conflict of interest regarding this work.

References

1. Bérard T, Cornet FH (2004) Evidence of thermally induced borehole elongation: a case study at Soultz, France. Int J Rock Mech Min Sci 41(5):883–883
2. Cai YY, Luo CH, Yu J, Zhang LM (2015) Experimental study on mechanical properties of thermal-damage granite rock under triaxial unloading confining pressure. Chin J Geotech Eng 37(7):1173–1180 **(in Chinese)**
3. Chamorro CR, Garciacuesta JL, Mondejar ME, Perezmadrazo A (2014) Enhanced geothermal systems in Europe: an estimation and comparison of the technical and sustainable potentials. Energy 65(2):250–263
4. Chen S, Yang C, Wang G (2017) Evolution of thermal damage and permeability of Beishan granite. Appl Therm Eng 110:1533–1542
5. Chen YL, Shao W, Zhou YC (2011) Experimental study on mechanical properties of granite after high temperature. Chin Q Mech 32(3):397–404 **(in Chinese)**
6. Chen YL, Ni J, Shao W, Azzam R (2012) Experimental study on the influence of temperature on the mechanical properties of granite under uni-axial compression and fatigue loading. Int J Rock Mech Min Sci 56(15):62–66
7. Chen YL, Wang SR, Ni J, Azzam R, Fernandez-steeger TM (2017) An experimental study of the mechanical properties of granite after high temperature exposure based on mineral characteristics. Eng Geol 220:234–242
8. Clark SP (1966) Handbook of physical constants. The Geological Society of America, Boulder
9. Du SJ, Liu H, Zhi HT, Chen HH (2004) Testing study on mechanical properties of post-high-temperature granite. Chin J Rock Mechan Eng 23(14):2359–2364 **(in Chinese)**
10. Fairhurst CE, Hudson JA (1999) Draft ISRM suggested method for the complete stress-strain curve for the intact rock in uniaxial compression. Int J Rock Mech Min Sci 36(3):279–289
11. Fan LF, Gao JW, Wu ZJ, Yang SQ, Ma GW (2018) An investigation of thermal effects on micro-properties of granite by X-ray CT technique. Appl Therm Eng 140:505–519
12. Fox DB, Sutter D, Beckers KF, Lukawski MZ, Koch DL, Anderson BJ, Tester JW (2013) Sustainable heat farming: modeling extraction and recovery in discretely fractured geothermal reservoirs. Geothermics 46(4):42–54
13. Ge ZL, Sun Q (2018) Acoustic emission (AE) characteristics of granite after heating and cooling cycles. Eng Fract Mech 200:418–429
14. Gónzalez-Gómez WS, Quintana P, May-Pat A, Avilés F, May-Crespo J, Alvarado-Gil JJ (2015) Thermal effects on the physical properties of limestone from the Yucatan Peninsula. Int J Rock Mech Min Sci 75:182–189
15. Homand-Etienne F, Houpert R (1989) Thermally induced microcracking in granites: characterization and analysis. Int J Rock Mech Min Sci Geomech Abstr 26(2):125–134
16. Hu SH, Zhang G, Zhang M, Jiang XL, Chen YF (2016) Deformation characteristics tests and damage mechanics analysis of Beishan granite after thermal treatment. Rock Soil Mech 37(12):3427–3436 **(in Chinese)**
17. Huang YH, Yang SQ, Tian WL, Zhao J, Ma D, Zhang CS (2017) Physical and mechanical behavior of granite containing pre-existing holes after high temperature treatment. Arch Civil Mech Eng 17(4):912–925
18. Jin PH, Hu YQ, Shao JX, Zhao GK, Zhou XZ, Li C (2019) Influence of different thermal cycling treatments on the physical, mechanical and transport properties of granite. Geothermics 78:118–128
19. Karakus GMN, Murthy CR (2001) Dual role of microcracks: toughening and degradation. Can Geotech J 38(2):427–440
20. Kumari WGP, Ranjith PG, Perera MSA, Shao S, Chen BK, Lashin A, Aeifi NAL, Rathnaweera TD (2017) Mechanical behaviour of Australian Strathbogie granite under in situ stress and temperature conditions: an application to geothermal energy extraction. Geothermics 65:44–59
21. Kumari WGP, Ranjith PG, Perera MSA, Chen BK, Abdulagatov IM (2017) Temperature-dependent mechanical behaviour of Australian Strathbogie granite with different cooling treatments. Eng Geol 229:31–44
22. Li B, Ju F (2018) Thermal stability of granite for high temperature thermal energy storage in concentrating solar power plants. Appl Therm Eng 138:409–416
23. Li ER, Wang YL, Chen L, Liu Y, Tan YH, Duan YH, Pu SK, Wang J (2018) Experimental study of mechanical properties of Beishan granite's thermal damage. J China Univ Min Technol 47(4):735–741 **(in Chinese)**
24. Liu S, Xu JY (2015) An experimental study on the physico-mechanical properties of two post-high-temperature rocks. Eng Geol 185(4):63–70
25. Lv C, Sun Q, Zhang WQ, Geng JS, Qi YM, Lu LL (2017) The effect of high temperature on tensile strength of sandstone. Appl Therm Eng 111:573–579
26. Martin-Gamboa M, Iribarren D, Dufour J (2015) On the environmental suitability of high- and low-enthalpy geothermal systems. Geothermics 53:27–37
27. Ozguven A, Ozcelik Y (2014) Effects of high temperature on physico-mechanical properties of Turkish natural building stones. Eng Geol 183:127–136
28. Peng J, Rong G, Cai M, Yao MD, Zhou CB (2016) Physical and mechanical behaviors of a thermal-damaged coarse marble under uniaxial compression. Eng Geol 200(12):88–93
29. Pranay A, Palash P, John ML, Joseph M (2019) Efficient workflow for simulation of multifractured enhanced geothermal systems (EGS). Renew Energy 131:763–777
30. Qiu YP, Lin ZY (2006) Testing study on damage of granite samples after high temperature. Rock Soil Mech 27(6):1005–1010 **(in Chinese)**
31. Rathnaweera TD, Ranjith PG, Gu X, Perera MSA, Kumari WGP, Wanniarachchi WAM, Haque A, Li JC (2018) Experimental investigation of thermomechanical behaviour of clay-rich

sandstone at extreme temperatures followed by cooling treatments. Int J Rock Mech Min Sci 107:208–223
32. Robinson E, Potter R, McInteer B, Rowley J, Armstrong D, Mills R (1971) Preliminary study of the nuclear subterrene. Los Alamos Scientific Lab, Los Alamos
33. Rong G, Peng J, Yao M, Jiang QH, Wong LNY (2018) Effects of specimen size and thermal-damage on physical and mechanical behavior of a fine-grained marble. Eng Geol 232:46–55
34. Rong G, Peng J, Cai M, Yao MD, Zhou CB, Sha S (2018) Experimental investigation of thermal cycling effect on physical and mechanical properties of bedrocks in geothermal fields. Appl Therm Eng 141:174–185
35. Shao SS, Wasantha PLP, Ranjith PG, Chen BK (2014) Effect of cooling rate on the mechanical behavior of heated Strathbogie granite with different grain sizes. Int J Rock Mech Min Sci 70(9):381–387
36. Shao SS, Ranjith PG, Wasantha PLP, Chen BK (2015) Experimental and numerical studies on the mechanical behaviour of Australian Strathbogie granite at high temperatures: an application to geothermal energy. Geothermics 54(54):96–108
37. Siratovich PA, Heap MJ, Villeneuve MC, Cole JW, Kennedy BM, Davidson J, Reuschlé T (2016) Mechanical behaviour of the rotokawa andesites (New Zealand): insight into permeability evolution and stress-induced behaviour in an actively utilised geothermal reservoir. Geothermics 64:163–179
38. Sirdesai NN, Singh TN, Ranjith PG (2017) Thermal alterations in the poro-mechanical characteristic of an Indian sandstone—a comparative study. Eng Geol 226:208–220
39. Tian H, Ziegler M, Kempka T (2014) Physical and mechanical behavior of claystone exposed to temperatures up to 1000°C. Int J Rock Mech Min Sci 70:144–153
40. Tian H, Mei G, Zheng MY (2016) The physical and mechanical properties of rocks after high temperature. China University of Geosciences Press, Wuhan **(in Chinese)**
41. Wu G, Zhai ST, Wang Y (2015) Research on characteristics of mesostructure and acoustic emission of granite under high temperature. Rock Soil Mech 36(Supp. 1):351–356 **(in Chinese)**
42. Xi BP, Zhao YS (2010) Experimental research on mechanical properties of water-cooled granite under high temperatures within 600 °C. Chin J Rock Mechan Eng 29(5):892–898 **(in Chinese)**
43. Xu C, Sun Q (2018) Effects of quenching cycle on tensile strength of granite. Géotech Lett 8(2):165–170
44. Xu XL, Gao F, Zhang ZZ (2014) Influence of confining pressure on deformation and strength properties of granite after high temperatures. Chin J Geotech Eng 36(12):2246–2252 **(in Chinese)**
45. Xu XL, Karakus M (2018) A coupled thermo-mechanical damage model for granite. Int J Rock Mech Min Sci 103:195–204
46. Yang SQ, Ranjith PG, Jing HW, Tian WL, Ju Y (2017) An experimental investigation on thermal damage and failure mechanical behavior of granite after exposure to different high temperature treatments. Geothermics 65:180–197
47. Yang SQ, Xu P, Li YB, Huang YH (2017) Experimental investigation on triaxial mechanical and permeability behavior of sandstone after exposure to different high temperature treatments. Geothermics 69:93–109
48. Yu J, Chen SJ, Chen X, Zhang YZ, Cai YY (2015) Experimental investigation on mechanical properties and permeability evolution of red sandstone after heat treatments. J Zhejiang Univ Sci A 16(9):749–759
49. Zhang WQ, Qian HT, Sun Q, Chen YH (2015) Experimental study of the effect of high temperature on primary wave velocity and microstructure of limestone. Environ Earth Sci 74(7):1–10
50. Zhang WQ, Sun Q, Hao SQ, Geng JS, Lv C (2016) Experimental study on the variation of physical and mechanical properties of rock after high temperature treatment. Appl Therm Eng 98:1297–1304
51. Zhang WQ, Sun Q, Zhu S, Wang B (2017) Experimental study on mechanical and porous characteristics of limestone affected by high temperature. Appl Therm Eng 110:356–362
52. Zhang JW, Chen X, Kang HY (2017) Experimental investigation of mechanical properties and energy features of granite after heat temperature under different loading paths. Tech Gazette 24(6):1841–1851
53. Zhao YS, Wan ZJ, Feng FJ, Xu ZH, Liang WG (2017) Evolution of mechanical properties of granite at high temperature and high pressure. Geomech Geophys Geo Energy Geo-Resour 3(2):1–12
54. Zhao ZH, Liu ZN, Pu H, Li X (2018) Effect of thermal treatment on Brazilian tensile strength of granites with different grain size distributions. Rock Mech Rock Eng 51(4):1–11
55. Zhi LP, Xu JY, Jin JZ, Liu S, Chen TF (2012) Research on ultrasonic characteristics and mechanical properties of granite under post-high temperature. Chin J Undergr Space Eng 8(4):716–721 **(in Chinese)**
56. Zhu D, Jing H, Yin Q, Han GS (2018) Experimental study on the damage of granite by acoustic emission after cyclic heating and cooling with circulating water. Processes 6:101